Exploiting Quantum Interference in Dye Sensitized Solar Cells

Emanuele Maggio,[†,*] Gemma C. Solomon,[‡,*] and Alessandro Troisi[†,*]

[†]Chemistry Department & Centre of Scientific Computing, University of Warwick, Coventry CV4 7AL, United Kingdom, and [‡]Nano-Science Center and Department of Chemistry, University of Copenhagen, Copenhagen 2100, Denmark

ABSTRACT A strategy to hinder the charge recombination process in dye sensitized solar cells is developed in analogy with similar approaches to modulate charge transport across nanostructures. The system studied is a TiO_2 (anatase)—chromophore interface, with an unsaturated carbon bridge connecting the two subunits. A theory for nonadiabatic electron transfer is employed in order to take explicitly into account the contribution from the bridge states mediating the process. If a cross-conjugated fragment is present in the bridge, it is possible to suppress the charge recombination by negative interference of the possible tunnelling path. Calculations carried out on realistic molecules at the DFT level of theory show how the recombination lifetime can be modulated by changes in the electron-withdrawing (donating) character of the groups connected to the cross-conjugated bridge. Tight binding calculations are employed to support the interpretation of the atomistic simulations.

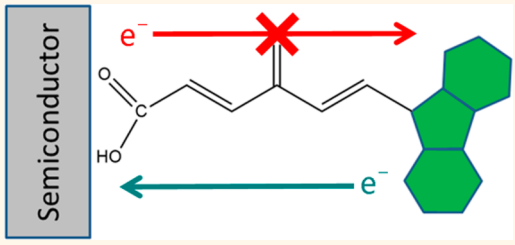

KEYWORDS: charge recombination · interface · semiconductor · tunnelling · antiresonance

In the field of dye sensitized solar cells (DSSCs), progressively more emphasis has been placed on the molecular characteristics of the constituents materials.[1] This trend can be associated with a more molecule-oriented description of the elementary steps in the charge conversion process: the sensitizer's chemical structure is known to impact on the electron injection and on the charge recombination processes.[2] The electron injection is initiated by the promotion of an electron on an excited state on the dye molecule which then injects it into the semiconductor conduction band, given a favorable energy alignment of the orbitals involved. The charge recombination reaction (CRR), which is a main dissipative pathway for DSSCs, can be described as the charge transfer from the semiconductors' conduction band to the lowest energy empty orbitals on the oxidized dye and it is in competition with the electron diffusion into the semiconductor electrode.

Two different approaches are available to curb the CRR: diminishing the concentration of either of the reactants or reducing the reaction rate constant of the process. The first approach can be implemented by increasing the electron mobility in the semiconductor, for instance by reducing the number of defects in the crystalline lattice, or by making the dye regeneration reaction faster. The reduction of defect states in the TiO_2 substrate has been studied experimentally[3,4] and chemical protocols have been devised to this end; however, this would also impact on the manufacturing cost of the device. One could decrease the concentration of the oxidized dye by accelerating the dye regeneration reaction, but the latter is already the most energetically wasteful process in conventional DSSCs (because of the driving force needed),[5] and therefore, increasing the driving force to make this reaction faster would further reduce the work extracted by the device (incidentally, moving the electrolyte level to higher energies, *i.e.*, closer to the TiO_2 conduction band edge, could also make the CRR to electrolyte species more favorable).[6]

For these reasons, the most advantageous strategy to reduce the CRR is to make this process inherently slower by a suitable design of the electronic structure of the dye. A typical approach[7] would lead to the design of sensitizers with a donor—acceptor structure, so that, in their excited state a partial charge transfer state would occur, with the injecting orbital localized as close as possible to the semiconductor surface and with the positive charge in the oxidized

* Address correspondence to e.maggio@warwick.ac.uk, gsolomon@nano.ku.dk, a.troisi@warwick.ac.uk.

Received for review September 2, 2013 and accepted November 27, 2013.

Published online 10.1021/nn4045886

state spatially removed from it. Alternatively, the orbital symmetry of the dye can be used to reduce the CRR by 2 to 3 orders of magnitude.[8] Herein, we suggest a different approach to reduce the CRR that is applicable when the dye is formed by a chromophore (the light harvesting unit) connected to a bridge that links it to the semiconductor surface. This type of structure is quite common among the organic dyes that have been employed in the field of DSSCs,[9] although the role of the bridge moiety has been typically limited to increasing the distance between the dye cation and the semiconductor surface and, in second instance, to extend the dye's absorption spectrum.[10] We explore an optimized design of the bridge portion that is able to slow down the charge recombination process, and might prove useful in the quest for more efficient DSSCs.

The CRR rate is computed for dyes featuring a cross-conjugated bridge and compared with the linear counterpart that is very common among DSSCs sensitizers.[9] A cross-conjugated molecule can be defined in general as "as a compound possessing three unsaturated groups, two of which although conjugated to a third unsaturated centre are not conjugated to each other".[11] In what follows we consider as a bridge a polyene chain made of sp^2 carbon atoms with a branching point (see Figure 1). The carbon atom at the branching point will be connected to a side group *via* a double bond and to two carbon atoms in the main backbone of the bridge *via* formally single bonds. The latter two atoms are therefore not conjugated as they are separated by two consecutive single bonds. Two molecular fragments are connected by a cross conjugated bridge when two consecutive single bonds between sp^2 carbons are found along the chain that connects the two fragments. This type of bridge has been extensively studied in the field of electron transport and their prominent characteristic is the occurrence of an antiresonance feature in the electronic transmission, *i.e.*, the transmission function through the bridge is negligible for incoming electrons in a well-defined energy window.[12] Furthermore, it has been shown how, by substituting the functional group attached to the branching point, it is possible to modulate the transmission properties by shifting the energy range at which the antiresonance occurs.[12] A recent study[13] has related the presence of this antiresonance to the topology of the π system, and has established a simple graphical rule to predict the presence of this quantum interference feature in the transmission function.

Cross-conjugated molecules are by no means the only molecular systems that exhibit destructive interference effects. There have been significant theoretical efforts over the last 15 years describing these effects in a range of molecules.[14−22] For example, the presence

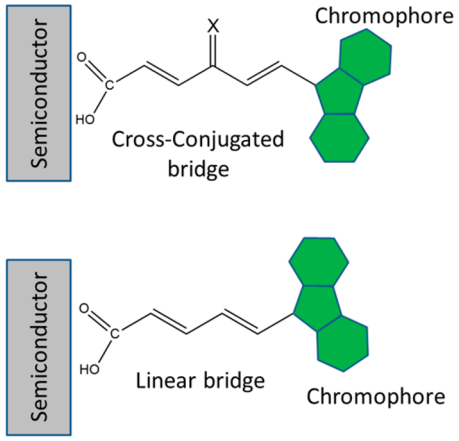

Figure 1. Sketches of dye molecules featuring a cross-conjugated bridge (top) and a linearly conjugated one (bottom).

of localized states energetically close to states strongly coupled to the electrodes gives rise to so-called Fano resonances, *i.e.*, peak-dip or dip-peak structures in the transmission function.[17,19] However, an interference feature able to prevent charge recombination should be ideally made only by a dip in the transmission function, a property commonly displayed by cross-conjugated molecules. Other chemical structures can be designed that would fulfill the same underlying principle: for example, meta-substituted cyclic systems (such as phenyl rings) or quinone-like structures are also suitable candidates for the approach we present. Recent experimental investigations of tunnelling transport[23] or transfer[24] are available, with the charge transfer being slower by a factor 30 in comparison with linearly conjugated systems. To the best of our knowledge, this idea has not been explored in the context of dye sensitized solar cell and can expand the already large application of theoretical chemistry to this problem.[25−28]

This work proceeds as follows: the theory of bridge mediated charge recombination is briefly reconsidered and it is then adapted to study the phenomenology of a simple model Hamiltonian. The results will then be generalized to the case of a realistic system, studied at the DFT level of theory.

RESULTS AND DISCUSSION

Bridge Mediated Charge Recombination. The model for bridge mediated charge recombination in DSSCs integrates the theory of electron transfer at electrochemical interfaces,[29−31] which we have recently applied to DSSC interfaces,[32] with the theory of electron tunnelling through molecular bridges developed for studies in photochemistry[33,34] and molecular junctions.[24,35]

If we consider a system that can be partitioned into semiconductor (S) bridge (B) and chromophore (M), then by labeling with *s*, *b*, and *m* the states from each partition, respectively, we can express the electronic

Hamiltonian as:

$$H = H_S + H_B + H_M + V_{SB} + V_{BM} \quad (1)$$

$$H_S = \sum_{s\in S} \varepsilon_s |s\rangle\langle s|;\ H_B = \sum_{b\in B} \varepsilon_b |b\rangle\langle b| + \sum_{b'\in B} \beta_{bb'} |b\rangle\langle b'|;$$

$$H_M = \varepsilon_m |m\rangle\langle m| \quad (2)$$

$$V_{SB} = \sum_{s,b} \tau_{sb} |s\rangle\langle b| + h.c.;$$

$$V_{BM} = \sum_{b\in B} \kappa_{bm} |b\rangle\langle m| + h.c \quad (3)$$

where the semiconductor's Hamiltonian term has been expressed in a diagonal representation for convenience. We indicate with τ and κ, respectively, the coupling matrix elements between semiconductor and chromophore orbitals with states on the bridge, while β is the coupling term between different bridge states. The electronic coupling between different subsystems is responsible for triggering the electron transfer; in the definition of the Hamiltonian operator, we have intentionally omitted the direct coupling between the semiconductor and the chromophore states as it decays exponentially with the distance between the two. The electronic states involved do not need to be mutually orthogonal; however, the partitioning of the total system given in eq 1 requires them to be localized on the respective subsystems. The expression for the charge recombination reaction rate stems from low-order perturbation theory and can be recast as:[32]

$$k_{CRR} = \int f_\mu(E) \tilde{\Gamma}(E) F(\varepsilon_m - E)\, dE \quad (4)$$

with the rate being proportional to the electron population in the semiconductor's conduction band (affected by the *quasi*-Fermi level position through the Fermi-Dirac distribution $f_\mu(E)$), to the spectral density $\tilde{\Gamma}(E)$, which accounts for the bridge mediated electronic coupling and to the Franck–Condon term $F(\varepsilon_m - E)$, described below. The density of electronic states in the semiconductor is included in the spectral density $\tilde{\Gamma}(E)$ through the definition:

$$\tilde{\Gamma}(E) = \frac{2\pi}{\hbar} \sum_s |\tilde{V}_{sm}| \delta(E - \varepsilon_s) \quad (5)$$

where the effective (bridge-mediated) electronic coupling between the semiconductor and the chromophore has been introduced.

The expression for the effective electronic coupling can be derived within the Lippmann-Schwinger formalism of scattering theory[36,37] or considering explicitly the equations of motion for the system:[38] the propagation mediated by (unperturbed) bridge states is then included thanks to the Green's function operator $g(E) \equiv (E - H_B)^{-1}$ to give $\tilde{V} = V_{SB} g V_{BM}$, where other terms have been previously defined in eq 3. Equipped with this definition, we can represent more explicitly the spectral density term as:[39]

$$\tilde{\Gamma}(E) = tr\{\mathbf{\Gamma g K g K}^\dagger\} \quad (6)$$

where $tr\{\bullet\}$ is the trace operator over the bridge states acting on the matrices involved. These are the following: the coupling between the semiconductor and the bridge ($\mathbf{\Gamma}$, defined below), the Green's function operator **g** and the coupling between the bridge and the chromophore unit (**K**). The matrices in eq 6 are related to the matrix elements defining the system as:

$$\Gamma_{ab}(E) = \frac{2\pi}{\hbar} \sum_s \tau_{as}^\dagger \tau_{sb} \delta(E - \varepsilon_s)$$

and $K_{cd} = \kappa_{dm} \kappa_{cm}^\dagger$. The bridge–chromophore coupling matrix elements are more conveniently expressed in terms of the atomic orbitals ϕ_j comprising the state m:

$$\kappa_{bm} = \sum_j c_j^m \langle b | V_{BM} | \phi_j \rangle$$

The structure of the manifold defining the initial and final states in the electron transfer process contains the vibrational contribution from the nuclear rearrangement taking place within the molecular subsystem and in the solvation sphere surrounding the system. The thermal occupation of the initial vibrational state will have to be included in the rate expression, together with the overlap between the different vibrational states accessible before and after the electron transfer. Furthermore, the underpinning assumption in adopting the scattering formalism is that the energy is conserved during the transition from the initial to the final state;[40] these different aspects are all taken into account by the Franck–Condon term, $F(\varepsilon_m - E)$, which represents the weighted density of nuclear states involved in the transition. In the semiclassical approximation, it can be evaluated as:

$$F(\varepsilon_m - E) = \frac{1}{\sqrt{4\pi\lambda k_B T}} \exp\left[-\frac{(\varepsilon_m - E + \lambda)^2}{4\lambda k_B T}\right] \quad (7)$$

with ε_m we indicate the free energy variation that the oxidized dye undergoes with the charge transfer and λ is the reorganization energy.[41]

The rate expression in eq 4 involves a sum over the energies of the incoming electrons present in the semiconductor. At each energy, the charge recombination rate is determined by the population of the electronic states $f_\mu(E)$, the Franck–Condon term and the spectral density $\tilde{\Gamma}$, which collects the information on the electronic structure of semiconductor–dye interface and the tunnelling probability across the bridge. For many realistic situations, only a narrow range of energies (within few $k_B T$ above the conduction band edge) will give a contribution to the rate. To minimize the charge recombination rate (without

affecting the charge injection), one should design a dye that has a minimum of $\tilde{\Gamma}(E)$ for energies close to the conduction band edge. In this respect, cross-conjugated bridges can be successfully employed to modulate the charge recombination rate, thanks to their antiresonance feature mentioned in the introduction.[12,24,35] The role of this antiresonance for charge recombination is shown in Figure 2. We will start by illustrating the proposed design with a tight binding model of the bridge moiety for linear and cross-conjugated bridges. These results will be compared with those obtained from a DFT simulation of the TiO_2−dye interface.

Charge Recombination through Tight Binding Linear and Cross-Conjugated Bridges. We initially consider a tight binding bridge model to explore the phenomenology in a fully controllable system, before considering a realistic case. If we indicate with N the total number of bridge states, which coincides with the number of bridge sites as shown in Figure 3, and allow only the terminal sites to interact with the semiconductor and the light harvesting unit, respectively, then the bridge Hamiltonian and the coupling terms become:

$$H_B = \sum_{b=1}^{N} \alpha_b |b\rangle\langle b| + E_X |X\rangle\langle X| + \sum_{b=1}^{N-1} \beta(|b\rangle\langle b+1| + |N-2\rangle\langle X|) + h.c.$$
$$V_{SB} + V_{BM} = \tau |s\rangle\langle 1| + \kappa |N\rangle\langle m| + h.c. \quad (8)$$

where $|X\rangle$ indicates the substituent group connected to the bridge over the cross-conjugated bond and E_X is the corresponding site energy, α_b is the on-site energy parameter for the remaining bridge sites while β is the tunnelling matrix element from one site to the next, the substituent is attached to the bridge at the site $N-2$. We consider cross-conjugated bridges of length $N = 5, 7$.

We describe the linearly conjugated system by removing the terms containing the cross-conjugated state $|X\rangle$ from eq 8 and setting $N = 6$.

If we assume a uniform distribution of semiconductor's states, ρ, above an energy threshold (which can be identified with the conduction band minimum), eq 6 can be simplified as:[42]

$$\tilde{\Gamma}(E) = \frac{2\pi}{\hbar} |\tau\kappa|^2 |G^0_{1,N}(E)|^2 \rho \quad (9)$$

where the only surviving element of the Green's operator is the one corresponding to the path connecting the first and the last bridge sites, and because of the choice made for the density of semiconductor states, the expression above will return a nonzero spectral density only for energies above the semiconductor's conduction band minimum. In eq 9, we have exploited the same assumptions made previously, with the bridge Green's function evaluated on the nonperturbed bridge states on the basis of weak

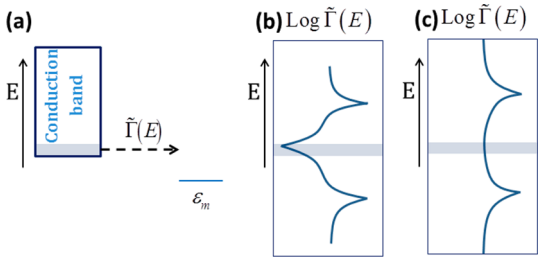

Figure 2. (a) Illustration of the energy levels for the electron transfer from the bottom of the conduction band of the semiconductor to the dye. A relatively narrow range of initial energies E is involved. The rate is controlled by the spectral density $\tilde{\Gamma}$ which depends on the nature of the bridge. Herein we design a bridge that contains an antiresonance (a minimum of $\tilde{\Gamma}$) in correspondence with the electron transfer energy, to minimize the rate of charge recombination. This is illustrated in (b), while the spectral density for a bridge without antiresonances is shown in (c).

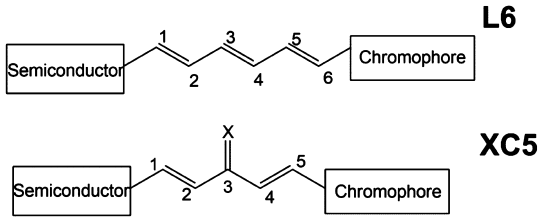

Figure 3. Sketches of the tight-binding systems considered.

coupling between bridge and semiconductor, while the interaction with the chromophore does not affect the spectral density in the energy range of interest. In this way, since the Green's function will depend only on the bridge's Hamiltonian, eq 9 contains well factorized the properties of the bridge and of its coupling with the semiconductor and the rest of the dye.

The Green's function is an analytic function in the complex plane, with isolated singularities corresponding to the eigenvalues of the Hamiltonian operator; we will refer to these peaks in the Green's function as resonances. The presence of resonances is the only type of behavior that the Green's function can show in a linear bridge. On the other hand, for cross conjugated systems, the occurrence of destructive quantum interference is also possible for specific energies of the incoming electron. This feature manifests as a vanishing probability of electron tunnelling across the bridge fragment at certain energies, and correspondingly, the Green's function will have a zero at those energies, *i.e.*, it will show an antiresonance.

The occurrence of an antiresonance in the XC5 cross-conjugated bridge is shown in Figure 4, where the absolute value of the Green's function is reported in panel a for an incoming electron entering the bridge through the first site and leaving through the last. The different Green's functions shown are obtained by varying the on-site energy E_X of the cross-conjugated substituent and an antiresonance occurs when the

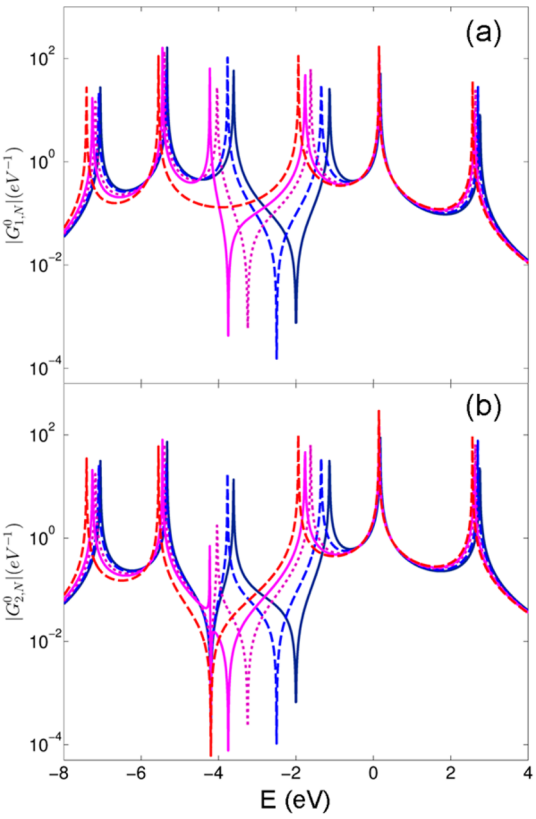

Figure 4. Green's functions for the XC5 bridge evaluated between the first and the terminal bridge sites (a) and between the second and the terminal site (b) for different values of E_X: −2.0 eV (solid blue), −2.5 eV (dashed blue), −3.25 eV (dotted purple), −3.75 eV (solid magenta) and −4.5 eV (dashed red). Tight binding parameters: $\alpha_b = -4.2$ eV for $b = 1$, $\alpha_b = -2.0$ eV otherwise, $\beta = -2.5$ eV.

energy variable matches the value E_X. This feature is suppressed when the energy E_X is aligned with a resonance of the bridge (as for the case of $E_X = -4.5$ eV, red dashed line).

In a real molecule, however, the coupling with the semiconductor can have a more complex structure than that postulated in this tight binding model: to illustrate on a simple system the type of feature observed in a realistic molecule, we consider a case where the coupling between the second bridge site and the semiconductor is different from zero, giving a finite probability for the electron to enter the bridge through this site. In this case, the Green's functions show a richer structure, as reported in Figure 4b. The tunnelling probability for the incoming electron vanishes at two different energy values; one of the two antiresonance features (the one occurring at higher energies) can still be modulated by modifying the value of the site connected to the cross-conjugated chain. When we progressively decrease the value of E_X, this antiresonance is shifted toward lower energies until it coalesces with the second antiresonance (located at the on-site energy value for the first site), which is not sensitive to the particular value of E_X

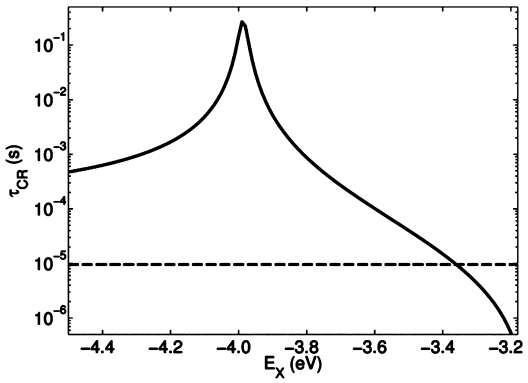

Figure 5. Charge recombination lifetime for the XC5 bridge as a function of the cross-conjugated group site energy. The value obtained for the linear bridge L6 is indicated by a dashed line.

employed. On the basis of this model, we can therefore expect that (at least some) antiresonance features occurring in realistic systems will be tunable by chemical means, *i.e.*, by replacing the chemical substituent attached to the cross-conjugated branching point.

To assess the impact of the cross-conjugated geometry on the bridge-mediated recombination rate, the spectral density is computed by setting tight binding parameters as specified in the Methods section, since this choice produces antiresonances near $E = -4.0$ eV, which is the lower energy threshold for the semiconductor's conduction band.

The charge recombination lifetime (computed as the reciprocal of the rate) is reported in Figure 5 as a function of the cross-conjugated on-site energy E_X for the bridge XC5 (solid line) and for the linear bridge L6 as a reference (dashed line). Results show that the recombination lifetime can be slowed down by 4 orders of magnitude if the antiresonance feature in the $G^0_{1,N}$ function is aligned with the conduction band edge. This characteristic of cross-conjugated bridges is very encouraging and justifies further investigation at a higher level of theory to confirm the results obtained and ascertain if this property is shared by more realistic systems.

Atomistic DFT Simulation of the Dye−TiO_2 Interface and Charge Recombination Evaluation. In this section, we explore the possibility of designing a realistic dye which, according to accurate DFT calculations, displays the same features identified in the tight binding model. We consider a cross-conjugated structure for the bridge moiety in the attempt to reproduce the increase in charge recombination lifetimes in the tight binding model. The chemical structures of the dyes considered are shown in Figure 6, with X indicating the substituent on the cross-conjugated chain.

The resulting $\tilde{\Gamma}$ is shown in Figure 7 for the cross-conjugated systems considered. Again, the energy axis has been shifted upward by 0.6 eV so that the calculated conduction band minimum E_C, estimated for the

isolated slab, has been aligned to its typical experimental value (−4.0 eV) in a DSSC.[43] The energy range which has the greatest impact on the recombination lifetime is highlighted by a dark marker, the lowest value in the highlighted region is the conduction band edge. This choice for the integration range is consistent with the assumption that (sub)surface trap states do not modify the relative semiconductor−bridge coupling. The assessment of this approximation is reported further on.

The spectral densities obtained from DFT calculations reproduce the behavior obtained from TB calculations in two respects: (i) chemical modification of the bridge structure shifts the position of the resonance associated with states localized on the bridge and (ii) antiresonance features occur at different values of E depending on the chemical substituent connected to the cross-conjugated group. Moreover, DFT calculations consistently identify an antiresonance (highlighted by the asterisk (*) symbol in Figure 7) that is not sensitive to the bridge chemical structure, as shown by the spectral densities reported in Figure 7 for electron withdrawing (left) and electron donating (right) groups. The eigenstates associated with the starred antiresonance are shown in Figure 8a,b for the L6 bridge. The states considered are mainly localized on the semiconductor, and they extend only on the anchoring group portion of the sensitizer; the two states show fairly different symmetries in this region. Since this antiresonance feature is associated with the nature of anchoring group alone, it is expected to be robust with respect to changes in the bridge structure. The origin of this antiresonance can be also due to the mechanism described, for example, in ref 19, where localized states are coupled to delocalized states.

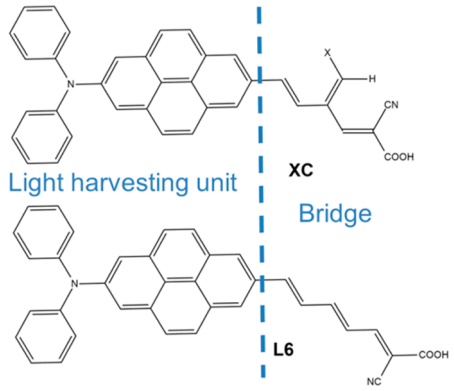

Figure 6. Chemical structures for the Pyrene derivatives employed in the DFT calculations. We set the cross-conjugated substituent X equal to: −NO_2, −CN, −COCl, −$COCH_3$, −CHO, −OH, −H, and −OCH_3.

Conversely, the resonances in Figure 7 that show a strong dependence on the substituent (*i.e.*, those located between −4.3 and −4.2 eV for the nitro, cyano and the acyl chloride substituents) are associated with states delocalized over the whole bridge, as shown by the lower panels in Figure 8. In some cases, this state produces a strong constructive interference effect when it approaches the relevant states localized on the anchoring group, possibly due to the orbital hybridization. This particular behavior is bound to increase spectral density in the energy region close to the conduction band edge, therefore accelerating the charge recombination process.

However, proceeding along the series of substituents with those reported in the right panel of Figure 7, we notice how also the antiresonance feature, originally located at −4.5 eV approximately for electron withdrawing groups is shifted toward higher energies. The antiresonance alignment observed for the −OH substituted bridge is particularly favorable since the spectral density is significantly depressed in an energy range of 0.3 eV near the conduction band edge, more than the interval of few k_BT relevant for the integral in eq 4.

In general, we can say that the calculation reveals the presence of antiresonances above and below the conduction band edge; some of these features are modulated by the energy of the side group, as predicted by the tight binding model analyzed in the previous section, while others stem from the topology of the specific anchoring group employed, hence are not reproduced by the tight binding approach.

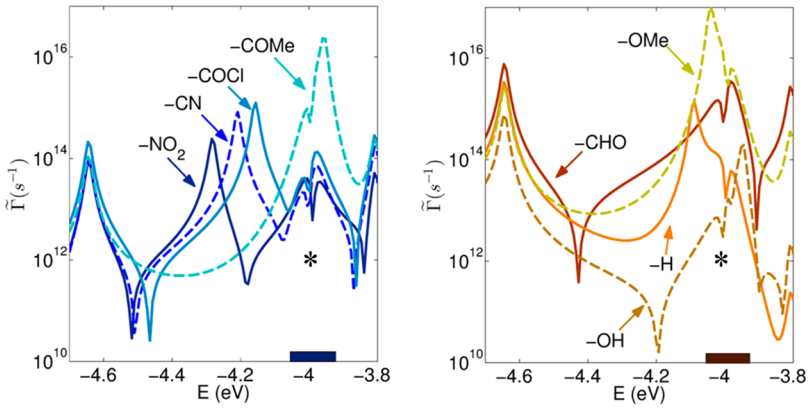

Figure 7. The bridge mediated semiconductor-dye coupling for electron withdrawing cross-conjugated groups (left panel) and for electron donating groups (right panel). The integration range is highlighted by a shaded area.

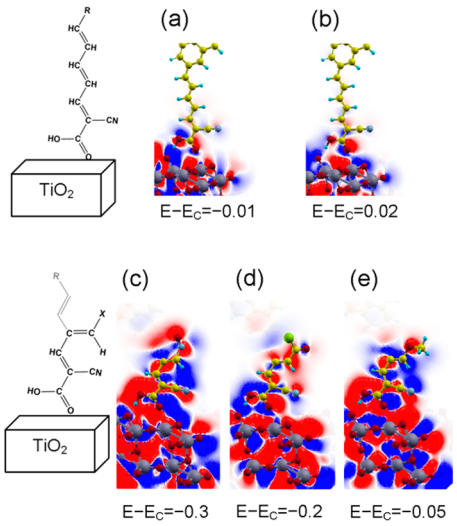

Figure 8. Wave functions sections in the plane containing the anchoring group for the linear bridge L6 (a) and (b), and for cross-conjugated bridges: $-NO_2$ (c), $-COCl$ (d), $-OCH_3$ (e). Corresponding energies are reported in eV. On the far left a sketch of the bridge's chemical structure is reported: with $-R$ we indicate the light harvesting unit shown in Figure 6 and the shaded portion refers to the fragment below the contour plot plane in panels c−e.

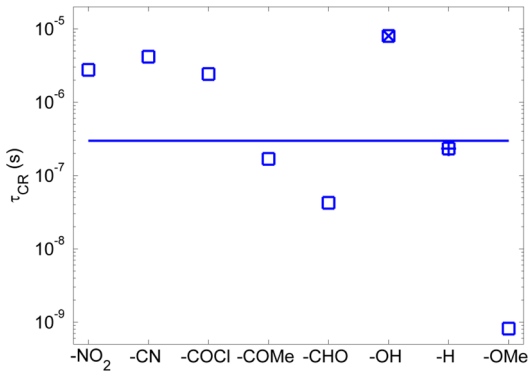

Figure 9. Charge recombination lifetimes for cross-conjugated molecules (with the lifetime for the linearly conjugated bridge L6 shown by a solid line), as a function of the chemical substituent. The symbols used for the −OH and −H substituents correspond to those used in Figure 10 below.

The values of charge recombination lifetimes are reported in Figure 9 and have been obtained by evaluating the rate over the conduction band energy range. The evaluation according to eq 4 implies that the recombination from trap states below the conduction band has been neglected and that equilibration of the electrons has been reached within the band in a time much shorter than the charge recombination time. Our theory can be extended to include recombination from localized states in the semiconductors,[44] but in the absence of detailed information about them, this generalization would increase the number of parameters in the model without affecting the essential result: antiresonances corresponding to the tunnelling energy will lower the recombination rate. However, while electron energy relaxation from the injection energy to the bottom of the conduction band is definitely faster than recombination rate (of the order of few ns),[45] the escape of the injected electrons from the interface region can be a slow process due to the presence of an exponential distribution of trap states.[46] Consequently, the measured electron lifetime, for example *via* impedance spectroscopy,[47] incorporates the dynamics of the electron within the traps and it does not correspond to the time computed by eq 4 which describes instead a single elementary process. The mismatch between the two times is of great importance for the correct interpretation of the device measurements,[48] but from the point of view of microscopic modeling, it is convenient to focus on the factors determining an individual elementary rate.

For the sake of completeness, we mention that many hypotheses have been put forward in literature concerning the microscopic origin of such trap states, and it was proposed that the Coulombic interaction between the oxidized dye and the electron in the band can create a localized hole−electron pair on the surface (charge transfer exciton).[49−51] In contrast with organic-based semiconductors, in high dielectric constant materials (such as TiO_2 nanoparticles), the role of electron−hole exchange effects is only relevant for the fine structure of low energy states and it is small enough to be treated as a perturbation.[52] Hence, Coulomb effects alone could suffice for an accurate picture of the charge transfer exciton. However, experimental evidence collected on the charge recombination reaction to oxidized dyes rules out a significant impact of these effects on the reaction rate.[53] A numerical study of the electron−hole pair (performed assuming that the electron can be considered a particle with the same effective mass of an electron in the semiconductor band, and that the dye is a point charge surrounded by a dielectric) estimated the exciton radius to be close to 200 Å and the exciton binding energy to be just 50 meV (using parameters appropriate for DSSC).[54] Therefore, it seems unlikely that hole−electron interaction can affect the results of this model significantly.

From the data in Figure 9 we can see how the introduction of a cross-conjugated bridge can slow down the charge recombination reaction by a factor 30 in comparison with the linear bridge L6 (shown in Figure 6). The information provided by the DFT simulation of the interface is richer than that provided by the minimal tight binding model for the (π electron mediated) charge transfer; however, some similarities exist. In particular, the profile observed for electron-donating groups is in qualitative agreement with the behavior for high values of the substituent on-site energy E_X. For these functional groups, there is a progressive increase in charge recombination lifetime, starting from the most electron-donating group, until a maximum is reached, corresponding to the −OH substituent. The reason for this slower charge recombination

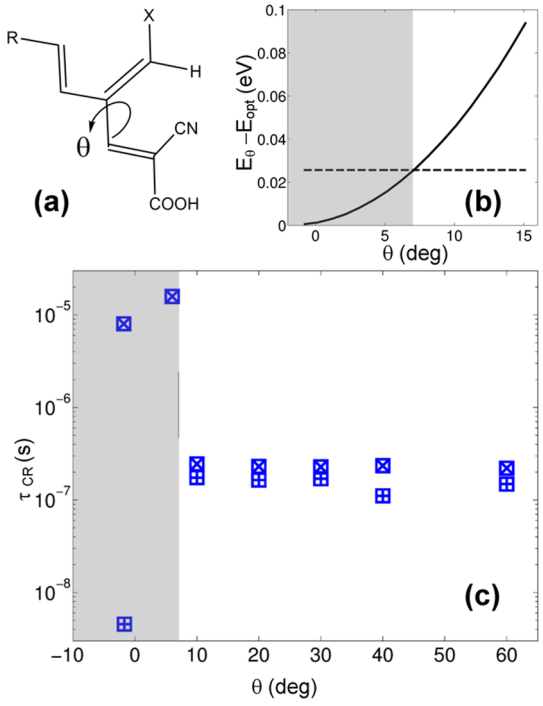

Figure 10. (a) Dihedral angle θ studied in the $-$OH and $-$H substituted bridges. (b) Energy scan for the $-$OH substituted molecule as a function of the dihedral angle, the thermal energy (T = 298.15 K) is marked by a dashed line. (c) Charge recombination lifetimes (τ_{CR}) for the $-$OH ($-$H) substituted bridge are marked with '$\times$' ('+') symbols, respectively; the shaded area highlights values for conformations accessible at room temperature.

has been ascribed to the presence of two antiresonances close to the energy window of interest. As these antiresonances move away (for the aldehyde substituent), the lifetime τ_{CR} decreases again, as predicted by the tight binding model. For electron-withdrawing groups (whose spectral densities are shown in the left panel of Figure 7), there is first suppression of the antiresonance (for the $-COCH_3$ group) and then the appearance of a feature showing an antiresonance near the conduction band minimum produces an increase in τ_{CR} that is not accounted for in the tight binding model.

Finally, we assess the robustness of the calculations on distortions of the dye's equilibrium geometry. We consider the dihedral angle (θ) between the cross-conjugated group and the rest of the bridge moiety shown in Figure 10a. Previous research on electron transmission has shown the relevance of this structural parameter on the electronic properties of the bridge studied.[19,35] The ground state energy is evaluated as a function of θ leaving the remaining nuclear degrees of freedom at their equilibrium values. The energy difference with the equilibrium conformation ($\theta = -1.8°$) is shown in panel b for the cross-conjugated bridge showing the slowest charge recombination lifetime (X = OH); this quantity is then evaluated over a range of θ values and reported in panel c together with τ_{CR} for the $-$H substituted cross-conjugated bridge.

Large distortions of the dihedral angle θ have a substantial impact on τ_{CR}: as shown in Figure 10c, a variation of more than 10° on the equilibrium value effectively 'isolates' the cross-conjugated group, giving an lifetime comparable with that obtained for a linearly conjugated bridge. However, the bridge structure is rather rigid, as shown by the span of θ accessible by interaction with a thermal bath in panel b; for values of θ in this range, the rate is left unaffected.

CONCLUSIONS

In this work, we have applied the theory of bridge mediated electron transfer in the attempt to impede the charge recombination reaction in dye sensitized solar cells. To this end, we have selected chromophores that feature a cross-conjugated bridge connecting the semiconductor with the light harvesting unit. We show that this class of molecules can be useful for the design of innovative sensitizers, since it is possible to modify with chemical means the intrinsic lifetime for one of the main dissipative pathways in the photon to electron conversion mechanism. The level of theory used precludes a definitive conclusion as to the optimal bridge structure because the exact alignment of molecular and seminconductor's level is subject to uncertainty.[55] However, it is clear that chemical substitution allows the charge recombination to be tuned over a significant range.

The theory allows us to rationalize the dependence of the charge recombination lifetime on the chemical nature of the bridge substituent in terms of the more prominent resonance and antiresonance features that most affect the spectral density near the semiconductor's conduction band edge. To help disentangle these features, a minimal tight binding model has complemented the description of the bridge's π-system electronic structure. Nuclear conformational effects have also been taken into account at the DFT level of theory; results are shown to be robust for distortions of the equilibrium conformation compatible with typical thermal energy values. The approach proposed in this paper can be added to the available strategies for the design of new sensitizers for solar cells or photocatalysis.

METHODS

Tight Binding Model. The Hamiltonian matrix for a cross-conjugated bridge has been constructed with a choice of the parameters in eq 8 of: $\alpha_b = -4.2$ eV for b = 1, $\alpha_b = -2.0$ eV otherwise, $\beta = -2.5$ eV; the on-site energy for the cross-conjugated group, E_X, has been varied as reported in Figure 4. The Green's function matrix is obtained by numerical inversion. The spectral density is obtained by setting κ = 0.25 eV, τ = 0.1 eV and $2\pi\rho \sim 1$ eV^{-1} in eq 9. The other parameters required to evaluate the charge recombination lifetime are the reorganization

energy λ and the free energy variation ε_m, together with the quasi-Fermi level μ inside the semiconductor. These values have been chosen as λ = 0.4 eV, $\varepsilon_m = -5.0$ eV, and $\mu = -4.1$ eV,[32] consistent with the values obtained from electronic structure calculations for the realistic dyes considered.

DFT Simulations. The electronic structure calculation for the evaluation of the spectral density in eq 6 proceeds in two steps: using the SIESTA code,[56] we have simulated independently the isolated TiO_2 slab and the whole system semiconductor + dye. The anatase (101) surface was modeled using a 3 × 3 surface supercell containing 108 atoms and four atomic layers. Geometry relaxation was performed while keeping the coordinates of the bottom atomic layer fixed at the values of the bulk phase. The Brillouin zone was then sampled with a cutoff parameter for the grid in the reciprocal space of 30 Å, the electronic structure was computed with a GGA-PBE exchange and correlation functional with double-ζ basis set and Troullier-Martins pseudopotentials. A similar geometry optimization was also carried out in presence of formic acid in order to establish the adsorption geometry of the dye's anchoring group. The rest of the dye molecule was attached to the carboxylic group preserving the relative orientation, and energy single point calculations were then performed at the same level of theory (including only the Γ-point on the slab + adsorbate system) in order to obtain the matrix elements of the full Hamiltonian operator. This last calculation was performed at the Γ-point only because we are not considering a periodic array of dyes interacting with each other, but rather only one dye adsorbed on a surface.

The semiconductor's Hamiltonian matrix H_S was obtained from the isolated slab calculation and it has been employed to evaluate the matrix elements Γ_{ab}. The simulation of the semiconductor + dye system allowed us to extract from the total Hamiltonian matrix the semiconductor−bridge and the bridge−chromophore coupling matrix elements (indicated with τ and κ, respectively, in the previous section), together with the bridge's Hamiltonian matrix H_B. The use of a localized basis set makes it possible to partition the dye molecule (and its Hamiltonian) into the bridge and chromophore fragments as required by our theoretical scheme. The chromophore fragment has been identified as the aromatic core in Figure 6, including the diphenilamino substituent; the bridge has been defined as the polyene chain including the carboxylic anchor and the cyano group attached to it. The coefficients of the molecular orbital on the chromophore fragment, indicated by c_j^m in the previous section, have been extracted from a similar single point energy calculation on the isolated dye. Reorganization energies and free energy variation have been evaluated on the solvated molecule (in acetonitrile) using the implicit solvation scheme adopted in our previous publication.[32]

Conflict of Interest: The authors declare no competing financial interest.

Acknowledgment. This work was supported by EPRSC and ERC.

REFERENCES AND NOTES

1. Listorti, A.; O'Regan, B.; Durrant, J. R. Electron Transfer Dynamics in Dye-Sensitized Solar Cells. *Chem. Mater.* **2011**, *23*, 3381–3399.
2. Clifford, J. N.; Martinez-Ferrero, E.; Viterisi, A.; Palomares, E. Sensitizer Molecular Structure-Device Efficiency Relationship in Dye Sensitized Solar Cells. *Chem. Soc. Rev.* **2011**, *40*, 1635–1646.
3. O'Regan, B.; Xiaoe, L.; Ghaddar, T. Dye Adsorption, Desorption, and Distribution in Mesoporous TiO_2 Films, and Its Effects on Recombination Losses in Dye Sensitized Solar Cells. *Energy Environ. Sci.* **2012**, *5*, 7203–7215.
4. O'Regan, B. C.; Durrant, J. R.; Sommeling, P. M.; Bakker, N. J. Influence of the $TiCl_4$ Treatment on Nanocrystalline TiO_2 Films in Dye-Sensitized Solar Cells. 2. Charge Density, Band Edge Shifts, and Quantification of Recombination Losses at Short Circuit. *J. Phys. Chem. C* **2007**, *111*, 14001–14010.
5. O'Regan, B. C.; Durrant, J. R. Kinetic and Energetic Paradigms for Dye-Sensitized Solar Cells: Moving from the Ideal to the Real. *Acc. Chem. Res.* **2009**, *42*, 1799–1808.
6. Bai, Y.; Zhang, J.; Zhou, D.; Wang, Y.; Zhang, M.; Wang, P. Engineering Organic Sensitizers for Iodine-Free Dye-Sensitized Solar Cells: Red-Shifted Current Response Concomitant with Attenuated Charge Recombination. *J. Am. Chem. Soc.* **2011**, *133*, 11442–11445.
7. Zeng, W.; Cao, Y.; Bai, Y.; Wang, Y.; Shi, Y.; Zhang, M.; Wang, F.; Pan, C.; Wang, P. Efficient Dye-Sensitized Solar Cells with an Organic Photosensitizer Featuring Orderly Conjugated Ethylenedioxythiophene and Dithienosilole Blocks. *Chem. Mater.* **2010**, *22*, 1915–1925.
8. Maggio, E.; Martsinovich, N.; Troisi, A. Using Orbital Symmetry to Minimize Charge Recombination in Dye-Sensitized Solar Cells. *Angew. Chem., Int. Ed.* **2013**, *52*, 973–975.
9. Mishra, A.; Fischer, M. K. R.; Bäuerle, P. Metal-Free Organic Dyes for Dye-Sensitized Solar Cells: From Structure: Property Relationships to Design Rules. *Angew. Chem., Int. Ed.* **2009**, *48*, 2474–2499.
10. Hara, K.; Kurashige, M.; Dan-oh, Y.; Kasada, C.; Shinpo, A.; Suga, S.; Sayama, K.; Arakawa, H. Design of New Coumarin Dyes Having Thiophene Moieties for Highly Efficient Organic-Dye-Sensitized Solar Cells. *New J. Chem.* **2003**, *27*, 783–785.
11. Phelan, N. F.; Orchin, M. Cross Conjugation. *J. Chem. Educ.* **1968**, *45*, 633–637.
12. Andrews, D. Q.; Solomon, G. C.; Van Duyne, R. P.; Ratner, M. A. Single Molecule Electronics: Increasing Dynamic Range and Switching Speed Using Cross-Conjugated Species. *J. Am. Chem. Soc.* **2008**, *130*, 17309–17319.
13. Markussen, T.; Stadler, R.; Thygesen, K. S. The Relation Between Structure and Quantum Interference in Single Molecule Junctions. *Nano Lett.* **2010**, *10*, 4260–4265.
14. Patoux, C.; Coudret, C.; Launay, J.-P.; Joachim, C.; Gourdon, A. Topological Effects on Intramolecular Electron Transfer via Quantum Interference. *Inorg. Chem.* **1997**, *36*, 5037–5049.
15. Collepardo-Guevara, R.; Walter, D.; Neuhauser, D.; Baer, R. A Hückel Study of the Effect of a Molecular Resonance Cavity on the Quantum Conductance of an Alkene Wire. *Chem. Phys. Lett.* **2004**, *393*, 367–371.
16. Walter, D.; Neuhauser, D.; Baer, R. Quantum Interference in Polycyclic Hydrocarbon Molecular Wires. *Chem. Phys.* **2004**, *299*, 139–145.
17. Ernzerhof, M.; Zhuang, M.; Rocheleau, P. Side-Chain Effects in Molecular Electronic Devices. *J. Chem. Phys.* **2005**, *123*, 134704.
18. Cardamone, D. M.; Stafford, C. A.; Mazumdar, S. Controlling Quantum Transport through a Single Molecule. *Nano Lett.* **2006**, *6*, 2422–2426.
19. Papadopoulos, T. A.; Grace, I. M.; Lambert, C. J. Control of Electron Transport through Fano Resonances in Molecular Wires. *Phys. Rev. B* **2006**, *74*, 193306.
20. Ke, S.-H.; Yang, W.; Baranger, H. U. Quantum-Interference-Controlled Molecular Electronics. *Nano Lett.* **2008**, *8*, 3257–3261.
21. Solomon, G. C.; Andrews, D. Q.; Goldsmith, R. H.; Hansen, T.; Wasielewski, M. R.; Van Duyne, R. P.; Ratner, M. A. Quantum Interference in Acyclic Systems: Conductance of Cross-Conjugated Molecules. *J. Am. Chem. Soc.* **2008**, *130*, 17301–17308.
22. Duchemin, I.; Renaud, N.; Joachim, C. An Intramolecular Digital 1/2-Adder with Tunneling Current Drive and Read-Outs. *Chem. Phys. Lett.* **2008**, *452*, 269–274.
23. Guedon, C. M.; Valkenier, H.; Markussen, T.; Thygesen, K. S.; Hummelen, J. C.; van der Molen, S. J. Observation of Quantum Interference in Molecular Charge Transport. *Nat. Nanotechnol.* **2012**, *7*, 305–309.
24. Ricks, A. B.; Solomon, G. C.; Colvin, M. T.; Scott, A. M.; Chen, K.; Ratner, M. A.; Wasielewski, M. R. Controlling Electron Transfer in Donor−Bridge−Acceptor Molecules Using Cross-Conjugated Bridges. *J. Am. Chem. Soc.* **2010**, *132*, 15427–15434.

25. Fantacci, S.; Angelis, F.; De, A. Computational Approach to the Electronic and Optical Properties of Ru(II) and Ir(III) Polypyridyl Complexes: Applications to DSC, OLED and NLO. *Coord. Chem. Rev.* **2011**, *255*, 2704–2726.
26. Labat, F.; Le Bahers, T.; Ciofini, I.; Adamo, C. First-Principles Modeling of Dye-Sensitized Solar Cells: Challenges and Perspectives. *Acc. Chem. Res.* **2012**, *45*, 1268–1277.
27. Martsinovich, N.; Troisi, A. Theoretical Studies of Dye-Sensitised Solar Cells: From Electronic Structure to Elementary Processes. *Energy Environ. Sci.* **2011**, *4*, 4473–4495.
28. Akimov, A. V; Neukirch, A. J.; Prezhdo, O. V Theoretical Insights into Photoinduced Charge Transfer and Catalysis at Oxide Interfaces. *Chem. Rev.* **2013**, *113*, 4496–4565.
29. Nitzan, A. *Chemical Dynamics in Condensed Phases: Relaxation, Transfer, and Reactions in Condensed Molecular Systems*; Oxford University Press:: Oxford, 2006; pp xxii, 719.
30. Chen, W.-C.; Marcus, R. A. Theory of a Single Dye Molecule Blinking with a Diffusion-Based Power Law Distribution. *J. Phys. Chem. C* **2012**, *116*, 15782–15789.
31. Schmickler, W.; Santos, E. *Interfacial Electrochemistry*; Springer:: Berlin, Heidelberg, 2010.
32. Maggio, E.; Martsinovich, N.; Troisi, A. Evaluating Charge Recombination Rate in Dye-Sensitized Solar Cells from Electronic Structure Calculations. *J. Phys. Chem. C* **2012**, *116*, 7638–7649.
33. Santabarbara, S.; Heathcote, P.; Evans, M. C. W. Modelling of the Electron Transfer Reactions in Photosystem I by Electron Tunnelling Theory: The Phylloquinones Bound to the PsaA and the PsaB Reaction Centre Subunits of PS I Are Almost Isoenergetic to the Iron−sulfur Cluster FX. *Biochim. Biophys. Acta, Bioenerg.* **2005**, *1708*, 283–310.
34. Blankenship, R. E.; Parson, W. W. The Photochemical Electron Transfer Reactions of Photosynthetic Bacteria and Plants. *Annu. Rev. Biochem.* **1978**, *47*, 635–653.
35. Solomon, G. C.; Andrews, D. Q.; Van Duyne, R. P.; Ratner, M. A. Electron Transport through Conjugated Molecules: When the π System Only Tells Part of the Story. *ChemPhysChem* **2009**, *10*, 257–264.
36. Taylor, J. R. *Scattering Theory*; John Wiley & Sons, Inc.: New York, 1972; p 477.
37. Emberly, E. G.; Kirczenow, G. Antiresonances in Molecular Wires. *J. Phys.: Condens. Matter* **1999**, *11*, 6911–6926.
38. Segal, D.; Nitzan, A.; Davis, W. B.; Wasielewski, M. R.; Ratner, M. A. Electron Transfer Rates in Bridged Molecular Systems 2. A Steady-State Analysis of Coherent Tunneling and Thermal Transitions†. *J. Phys. Chem. B* **2000**, *104*, 3817–3829.
39. Meir, Y.; Wingreen, N. S. Landauer Formula for the Current through an Interacting Electron Region. *Phys. Rev. Lett.* **1992**, *68*, 2512–2515.
40. Ziman, J. M. *Elements of Advanced Quantum Theory*; Cambridge University Press:: Cambridge, U.K.; New York, 1969; p 269.
41. Gao, Y. Q.; Georgievskii, Y.; Marcus, R. A. On the Theory of Electron Transfer Reactions at Semiconductor Electrode/Liquid Interfaces. *J. Chem. Phys.* **2000**, *112*, 3358–3369.
42. Mujica, V.; Kemp, M.; Ratner, M. A. Electron Conduction in Molecular Wires. I. A Scattering Formalism. *J. Chem. Phys.* **1994**, *101*, 6849–6855.
43. Fabregat-Santiago, F.; Garcia-Belmonte, G.; Mora-Sero, I.; Bisquert, J. Characterization of Nanostructured Hybrid and Organic Solar Cells by Impedance Spectroscopy. *Phys. Chem. Chem. Phys.* **2011**, *13*, 9083–9118.
44. Maggio, E.; Troisi, A. Theory of the Charge Recombination Reaction at the Semiconductor-Adsorbate Interface in the Presence of Defects. *J. Phys. Chem. C* **2013**, *117*, 24196–24205.
45. Sá, J.; Friedli, P.; Geiger, R.; Lerch, P.; Rittmann-Frank, M. H.; Milne, C. J.; Szlachetko, J.; Santomauro, F. G.; van Bokhoven, J. A.; Chergui, M.; *et al.* Transient Mid-IR Study of Electron Dynamics in TiO_2 Conduction Band. *Analyst* **2013**, *138*, 1966–1970.
46. Barnes, P. R. F.; Anderson, A. Y.; Durrant, J. R.; O'Regan, B. C. Simulation and Measurement of Complete Dye Sensitised Solar Cells: Including the Influence of Trapping, Electrolyte, Oxidised Dyes and Light Intensity on Steady State and Transient Device Behaviour. *Phys. Chem. Chem. Phys.* **2011**, *13*, 5798–5816.
47. Ondersma, J. W.; Hamann, T. W. Impedance Investigation of Dye-Sensitized Solar Cells Employing Outer-Sphere Redox Shuttles. *J. Phys. Chem. C* **2009**, *114*, 638–645.
48. Bisquert, J.; Fabregat-Santiago, F.; Mora-Seró, I.; Garcia-Belmonte, G.; Giménez, S. Electron Lifetime in Dye-Sensitized Solar Cells: Theory and Interpretation of Measurements. *J. Phys. Chem. C* **2009**, *113*, 17278–17290.
49. Peter, L. Sticky Electrons" Transport and Interfacial Transfer of Electrons in the Dye-Sensitized Solar Cell. *Acc. Chem. Res.* **2009**, *42*, 1839–1847.
50. Gregg, B. A. Excitonic Solar Cells. *J. Phys. Chem. B* **2003**, *107*, 4688–4698.
51. Yu, Q.; Wang, Y.; Yi, Z.; Zu, N.; Zhang, J.; Zhang, M.; Wang, P. High-Efficiency Dye-Sensitized Solar Cells: The Influence of Lithium Ions on Exciton Dissociation, Charge Recombination, and Surface States. *ACS Nano* **2010**, *4*, 6032–6038.
52. Scholes, G. D. Insights into Excitons Confined to Nanoscale Systems: Electron−Hole Interaction, Binding Energy, and Photodissociation. *ACS Nano* **2008**, *2*, 523–537.
53. Tachibana, Y.; Haque, S. A.; Mercer, I. P.; Durrant, J. R.; Klug, D. R. Electron Injection and Recombination in Dye Sensitized Nanocrystalline Titanium Dioxide Films: A Comparison of Ruthenium Bipyridyl and Porphyrin Sensitizer Dyes. *J. Phys. Chem. B* **2000**, *104*, 1198–1205.
54. Maggio, E. Theory of the Charge Recombination Rate in Dye Sensitised Solar Cells. Ph. D. Dissertation, University of Warwick, Coventry, UK, 2013, pp 157−166.
55. Pastore, M.; Fantacci, S.; De Angelis, F. Modeling Excited States and Alignment of Energy Levels in Dye-Sensitized Solar Cells: Successes, Failures, and Challenges. *J. Phys. Chem. C* **2013**, *117*, 3685–3700.
56. Soler, J. M.; Artacho, E.; Gale, J. D.; García, A.; Junquera, J.; Ordejón, P.; Sánchez-Portal, D. The SIESTA Method for *ab Initio* Order—N Materials Simulation. *J. Phys.: Condens. Matter* **2002**, *14*, 2745–2779.